Applied Mathematical Modelling 36 (2012) 2926–2934

Contents lists available at SciVerse ScienceDirect

Applied Mathematical Modelling

journal homepage: www.elsevier.com/locate/apm

# A numerical method to determine mode content in circular waveguide based on an integral identity equation

Simin Li [a], Zhibin Zhu [b,*]

[a] Faculty of Electrical Engineering and Automation, Guilin University of Electronic Technology, Guilin 541004, PR China
[b] Faculty of Mathematics and Computing Science, Guilin University of Electronic Technology, Guilin 541004, PR China

ARTICLE INFO

*Article history:*
Received 25 October 2010
Received in revised form 13 September 2011
Accepted 21 September 2011
Available online 2 October 2011

*Keywords:*
Open-ended circular waveguide
Mode of waveguide
Plane wave spectrum
Orthogonal integral identity equation
Numerical method

ABSTRACT

According to the orthogonality of circular waveguide modes, an orthogonal integral identity equation is proposed among plane-wave spectrum of different modes, under the same azimuthal angle index. By using this identity equation, a simple method, which can determine components of different modes, is proposed. In the end, some numerical experiment results are also reported, which show that the proposed method is efficient.



## 1. Introduction

In order to enhance the power capacity, the over-mode waveguide is always used to excite and propagated the multimode radiation in high power microwave sources. Because these waveguide modes frequently do not provide a suitable field configuration for the intended application, it is important to identify the mode content of the propagating waves for clarifying what modes are present, and whether the propagated mode meets the requirements. Usually, for an open end circular waveguide, it is the difficult work to discriminate the mode content at the plane of $z = 0$, by taking advantage of the plane-wave spectrum of the radiation of circular waveguide.

A number of techniques of mode content determination of highly over-mode waveguide are being utilized by the scientists and engineers. They include: scanning the field pattern methods [1,2]; selective mode couplers methods [3–5]; array processing methods [6–8]; measuring open end radiation pattern methods [9–13]; wavenumber spectrometer methods [14,15], etc. We refer to [16] for an excellent survey on this topic.

For scanning the field pattern methods, in [1], by employing some small calibrated probes, a theoretical analysis and experimental method was proposed to determine the power level and relative phase of each of several simultaneously propagating high order modes in a rectangular waveguide system. However, the total number of probe locations must be at least equal to,or usually more than the number of propagating modes. Moreover, in order to take the probe data, many multimode measurement procedure were required, which in turn imposed severe long-term requirements on the over-all system stability. In [2], according to some observable data with a conventional single mode network analyzer, an iterative method was proposed to evaluate the scattering parameters in a multi-mode waveguide. Of course, if it was not convergent for the infinite geometric series of the inverse matrix corresponding to multiple scatting, the algorithm was invalid.

* Corresponding author. Tel.: +86 13768747879; fax: +86 07732290700.
*E-mail addresses:* zhuzbma@hotmail.com, zhuzb@guet.edu.cn (Z. Zhu).

0307-904X/$ - see front matter © 2011 Elsevier Inc. All rights reserved.
doi:10.1016/j.apm.2011.09.067

For selective mode couplers methods, in [3], a simple and direct approach was proposed to discriminate different modes for a multi-mode measurement, by using the mode couplers which couple selectively to any desired mode. It seemed that the applications of these couplers was limited to systems in which the number of propagating modes is small. In [4], based on a multi-port scatting parameter measurements, an original multi-mode thru-reflection line calibration procedure was proposed to analyze multi-mode waveguide. However, its computational cost was large, and it was referred to as the "two-step calibration procedure", as the measurement system was calibrated twice. In [5], based on mode-selective coupling, a design and calibration method of mode discriminators was presented. The design examples for the case of equal-intensity coupling showed that this method was useful, and increasing the groups of coupling holes may suppress more unwanted modes and improve the properties of the mode discriminator. It should be noted that, by making use of this method, the operating frequency region of the designed mode discriminator was narrow.

For array processing methods, in [6], based on an array of field probes at the surface of an over-mode circular waveguide, a mode analyzer is described to handle dozens of modes. In [7], it was proposed a set of measurements by inserting a small loop probe into a number of locations in circular waveguide, and applied to determine relative mode amplitudes in a large over-mode waveguide. In [8], based on measuring the frequency response between the two antennas coupled into a waveguide, and using that information to extract the mode content generated by the transmitting antenna, a novel technique was present for analyzing the mode content excited by antennas placed in multi-mode waveguide. Nevertheless, these methods were not easy to implement for high power microwave waveguide.

For measuring open end radiation pattern methods, in [9,10], the modes were discriminated by analyzing the far field pattern of the multi-mode wave propagating in the microwave system. Here, the process must be repeated in an iterative manner until the mode content was identified successfully, if the calculated result of the pattern was not in agreement with the measured pattern. In [11], firstly, all of the propagating modes were grouped into some families with the same azimuthal dependence, for example, the $TE_{1n}$, $TE_{2n}$, $TM_{0n}$ families, and so on. Then, according to the characteristic that the zero points were different for different modes in the same family, each mode was discriminated one by one through open-end radiation pattern measurement. It must be also repeated several times measurements to identify successfully the mode content. In [12], based on the voltage traveling wave ratio equations, a technique was described for measurement of the voltage traveling wave ratios in multi-mode waveguides. Such measurements provide information necessary for design of multi-mode waveguide components and integration of such components into complex multi-mode systems. In [13], based on the intensity measurements and iterative synthesis of phase fronts of the radiation field, another waveguide field measuring method was suggested to probe the waveguide field directly inside the over-mode waveguide in a few cross sections. However, for both methods, the complicated measuring and calculating procedures were laborious and time consuming.

As already mentioned, some disadvantages were characteristic for the field measuring methods. To overcome these difficulties, the wave-number spectrometer was developed in [14,15]. In this instrument, the free-space radiation of an axial array of equidistant holes in the waveguide wall was used for mode analysis. The axial distance between the holes was less than a half free-space wavelength. This kind of method separated spatially the radiated direction of different modes using dispersive reflector antenna or leaky-wave antenna. As it was pointed out in [13,17], these methods were relatively complicated and require special setups. Most importance is that these methods, as a rule, measure the amplitudes of modes only. So, it was limited a capability of their application (complexity and difficulties of manufacturing growing with increase of frequency, narrow frequency band, insufficient resolving ability at definition of high types of modes close on a structure).

While, in [18], it was proposed an inner-product method. There, a radiation matrix was defined by using the inner-product, and modes components were determined by solving a system of linear equations. Since it was only necessary to compute the integral in two main axis, that method reduced the cost of measurement data. But, the scale and the framework of the system of linear equations were not known previously, since we did not know previously how many and which modes exist. Furthermore, when the integral was computed, due to the truncation of the elevation angle, there was the truncation error.

In this paper, using the orthogonality of circular waveguide modes, we firstly derive the orthogonal relation with far field plane-wave spectrum of open end circular waveguide. Then, through detailed analysis, we obtain an important orthogonal integral identity equation among plane-wave spectrum of different modes, under the same azimuthal angle index. Using this identity equation, we propose a simple method to determine different modes components, under the same azimuthal angle index. In the end, some numerical experiment results are also reported, which show that the proposed method is efficient.

The plan of the paper is as follows: in Section 2, the orthogonal properties of plane-wave spectrum is stated. In Section 3, we obtain an orthogonal integral identity equation among plane-wave spectrum of different modes. The numerical method is proposed in Section 4. And, in Section 5, some numerical experiments are implemented. Finally, the conclusion is given in Section 6.

## 2. The orthogonal properties of plane-wave spectrum

Assume that an open end circular waveguide located on the plane of $z = 0$ with axis aligning $z$ dimension and radius of $a$ (see Fig. 1). We analyze and calculate the aperture far field of this aperture by using the plane-wave spectrum approach [19].

For this open-end circular waveguide, the far field of this aperture can be represented by plane wave spectrum $\vec{f}_t(k_x, k_y)$ as follows [20]:

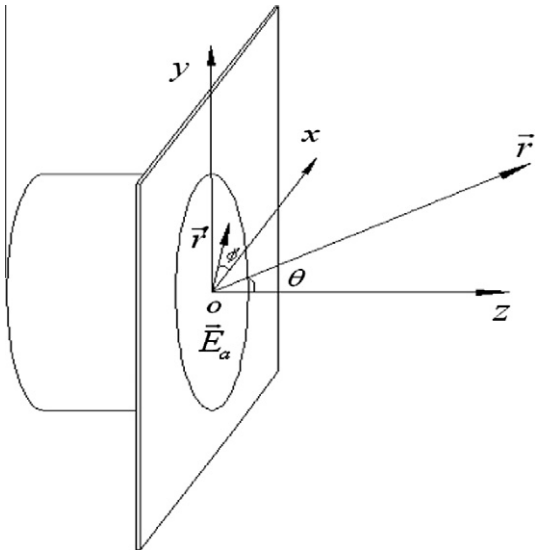


**Fig. 1.** Open-end circular waveguide.

$$\vec{E}(\vec{r}) \approx jk_0 \frac{\cos\theta e^{-jk_0 r}}{2\pi r} \vec{f}_t(k_0 \sin\theta\cos\phi', k_0 \sin\theta \sin\phi'), \tag{1}$$

moreover, the aperture field $\vec{E}_a(x,y)$ and its plane wave spectrum of the radiation far field $\vec{f}_t(k_x,k_y)$ are a Fourier transform pair as follows [19]:

$$\begin{aligned} \vec{f}_t(k_x,k_y) &= \int\int_{S_a} \vec{E}_a(x,y) e^{jk_x x + k_y y} dxdy, \\ \vec{E}_a(x,y) &= \frac{1}{4\pi^2} \int_{-\infty}^{\infty}\int_{-\infty}^{\infty} \vec{f}_t(k_x,k_y) e^{-j(k_x x + k_y y)} dk_x dk_y, \end{aligned} \tag{2}$$

where $k_x = k_0 \sin\theta\cos\phi'$, $k_y = k_0 \sin\theta\sin\phi'$, $(k_x,k_y)$ the propagation vector, $\phi'$ the azimuthal angle, and $\theta$ the elevation angle.

Let $E(x,y)$ consist of the sum incident circular waveguide modes. Assume that $\vec{e}_n(x,y)$ is the vector field function of the $n$th eigenmode, and $a_n$ is the corresponding argument, then we have that

$$\vec{E}_a(x,y) = \sum_{n=1}^{N} a_n \vec{e}_n(x,y). \tag{3}$$

Since eigenmodes of the metal waveguide are orthogonal, that is to say,

$$\int_{S_a} \vec{e}_n(x,y) \cdot \vec{e}_m^*(x,y) dS = \begin{cases} 1, & n = m, \\ 0, & n \neq m, \end{cases}$$

we can obtain that

$$a_n = \int_{S_a} \vec{E}_a(x,y) \cdot \vec{e}_n(x,y) dS. \tag{4}$$

Given two vector field functions of eigenmodes $\vec{e}_n(x,y)$ and $\vec{e}_m(x,y)$, denote that $\vec{f}_{tn}(k_x,k_y)$ and $\vec{f}_{tm}(k_x,k_y)$ are their corresponding plane wave spectrums, respectively. From Parseval formula, we obtain the following orthogonal properties of plane-wave spectrum:

$$\frac{1}{4\pi^2} \int_{-\infty}^{\infty}\int_{-\infty}^{\infty} \vec{f}_{tn}(k_x,k_y) \cdot \vec{f}_{tm}^*(k_x,k_y) dk_x dk_y = \begin{cases} 1, & n = m, \\ 0, & n \neq m. \end{cases} \tag{5}$$

## 3. The identity equation

For the sake of simplicity, in the sequel, we only analyze the case with the circular waveguide $TE_{mn}$ mode.

Under circular cylindrical coordinate system $(\rho,\phi,z)$, the electric field distribution of $TE_{mn}$ mode can be represented as follows [21]:

$$\begin{aligned} E_\rho &= N_{mn} m \frac{J_m(k_{\rho n}\rho)}{\rho} \sin m\phi, \\ E_\phi &= N_{mn} k_{\rho n} J'_m(k_{\rho n}\rho) \cos m\phi, \end{aligned} \tag{6}$$

where

$$N_{mn} = \sqrt{\frac{\varepsilon_m}{\pi}} \frac{1}{J_m(\chi_n)\sqrt{\chi_n^2 - m^2}}, \quad k_{\rho n} = \frac{\chi_n}{a}, \quad \varepsilon_m = \begin{cases} 1, & m = 0 \\ 2, & m \neq 0 \end{cases},$$

and $\chi_n$ is the $n$th non-zero root of the derivation of the $m$th-order Bessel function, $k_{\rho n}$ the cutoff wave-number of the circular waveguide.

In order to derive the expression of plane-wave spectrum, (6) is transferred under Cartesian coordinate system as follows:

$$\begin{aligned} E_x &= E_\rho \cos\phi - E_\phi \sin\phi, \\ E_y &= E_\rho \sin\phi + E_\phi \cos\phi. \end{aligned} \tag{7}$$

**Lemma 1.** *Under Cartesian coordinate system, the electric field distribution of the $TE_{mn}$ mode is expressed as follows:*

$$\begin{aligned} E_x &= \frac{N_{mn} k_{\rho n}}{2} [J_{m-1}(k_{\rho n}\rho)\sin(m-1)\phi + J_{m+1}(k_{\rho n}\rho)\sin(m+1)\phi], \\ E_y &= \frac{N_{mn} k_{\rho n}}{2} [J_{m-1}(k_{\rho n}\rho)\cos(m-1)\phi - J_{m+1}(k_{\rho n}\rho)\cos(m+1)\phi]. \end{aligned} \tag{8}$$

**Proof.** From (6) and (7), we have that

$$\begin{aligned} E_x &= E_\rho \cos\phi - E_\phi \sin\phi = N_{mn} m \frac{J_m(k_{\rho n}\rho)}{\rho} \sin m\phi \cos\phi - N_{mn} k_{\rho n} J'_m(k_{\rho n}\rho) \cos m\phi \sin\phi \\ &= N_{mn} m \frac{J_m(k_{\rho n}\rho)}{\rho} \left[\frac{1}{2}\sin(m+1)\phi + \frac{1}{2}\sin(m-1)\phi\right] - N_{mn} k_{\rho n} J'_m(k_{\rho n}\rho)\left[\frac{1}{2}\sin(m+1)\phi - \frac{1}{2}\sin(m-1)\phi\right]. \end{aligned}$$

Using following recurrence relationships of Bessel function $J_m(u)$:

$$J'_m(u) = \frac{1}{2}[J_{m-1}(u) - J_{m+1}(u)],$$

$$\frac{m}{n} J_m(u) = \frac{1}{2}[J_{m-1}(u) + J_{m+1}(u)],$$

it holds that

$$\begin{aligned} E_x &= \frac{1}{2} N_{mn} \sin(m+1)\phi \left\{ k_{\rho n} \frac{1}{2}[J_{m-1}(k_{\rho n}\rho) + J_{m+1}(k_{\rho n}\rho)] - k_{\rho n} \frac{1}{2}[J_{m-1}(k_{\rho n}\rho) - J_{m+1}(k_{\rho n}\rho)] \right\} \\ &\quad + \frac{1}{2} N_{mn} \sin(m-1)\phi \left\{ k_{\rho n} \frac{1}{2}[J_{m-1}(k_{\rho n}\rho) + J_{m+1}(k_{\rho n}\rho)] + k_{\rho n} \frac{1}{2}[J_{m-1}(k_{\rho n}\rho) - J_{m+1}(k_{\rho n}\rho)] \right\} \\ &= \frac{N_{mn} k_{\rho n}}{2} [J_{m-1}(k_{\rho n}\rho)\sin(m-1)\phi + J_{m+1}(k_{\rho n}\rho)\sin(m+1)\phi]. \end{aligned}$$

With the same reason, it is easy to obtain that

$$E_y = \frac{N_{mn} k_{\rho n}}{2} [J_{m-1}(k_{\rho n}\rho)\cos(m-1)\phi - J_{m+1}(k_{\rho n}\rho)\cos(m+1)\phi].$$

The proof is finished. □

**Lemma 2.** *Under Cartesian coordinate system, if m is odd, i.e., m = 2k − 1, k = 1,2,3,..., then the plane-wave spectrum of $TE_{mn}$ mode is expressed as follows:*

$$f_x = -\frac{N_{mn} u^2 v a \pi}{u^2 - v^2} \left\{ (-1)^k \sin 2(k-1)\phi' \left[ J'_{2(k-1)}(v) \frac{J_{2(k-1)}(u)}{u} - J'_{2(k-1)}(u) \frac{J_{2(k-1)}(v)}{v} \right] - (-1)^k \sin 2k\phi' \left[ J'_{2k}(v) \frac{J_{2k}(u)}{u} - J'_{2k}(u) \frac{J_{2k}(v)}{v} \right] \right\}, \tag{9}$$

$$f_y = -\frac{N_{mn}u^2 va\pi}{u^2 - v^2}\left\{(-1)^k \cos 2(k-1)\phi'\left[J'_{2(k-1)}(v)\frac{J_{2(k-1)}(u)}{u} - J'_{2(k-1)}(u)\frac{J_{2(k-1)}(v)}{v}\right] + (-1)^k \cos 2k\phi'\left[J'_{2k}(v)\frac{J_{2k}(u)}{u} - J'_{2k}(u)\frac{J_{2k}(v)}{v}\right]\right\}, \quad (10)$$

*where* $u = k_{\rho n}a$, $v = k_0 a \sin\theta$.

**Proof.** Firstly, from (2), we have, under circular cylindrical coordinate system, that

$$\vec{f}_t(k_x, k_y) = \int_0^a \int_0^{2\pi} \vec{E}_a(x,y) e^{jk_0\rho\sin\theta\cos(\phi-\phi')}\rho d\rho d\phi. \quad (11)$$

while, by using Taylor series, it holds that

$$e^{jk_0\rho\sin\theta\cos(\phi-\phi')} = J_0(k_0\rho\sin\theta) - 2\sum_{t=1}(-1)^{t+1}J_{2t}(k_0\rho\sin\theta)\cos 2t(\phi-\phi') + 2j\sum_{t=1}(-1)^{t-1}J_{2t-1}(k_0\rho\sin\theta)\cos(2t-1)(\phi-\phi'). \quad (12)$$

Substituting (8) and (12) into (11), due to the orthogonal characteristic of triangular function, it is easy to obtain that

$$f_x = N_{mn}k_{\rho n}\pi\left[(-1)^k \sin 2(k-1)\phi' \int_0^a J_{2(k-1)}(k_{\rho n}\rho)J_{2(k-1)}(k_0\rho\sin\theta)\rho d\rho + (-1)^k \sin 2k\phi' \int_0^a J_{2k}(k_{\rho n}\rho)J_{2k}(k_0\rho\sin\theta)\rho d\rho\right], \quad (13)$$

and

$$f_y = N_{mn}k_{\rho n}\pi\left[(-1)^k \cos 2(k-1)\phi' \int_0^a J_{2(k-1)}(k_{\rho n}\rho)J_{2(k-1)}(k_0\rho\sin\theta)\rho d\rho + (-1)^k \cos 2k\phi' \int_0^a J_{2k}(k_{\rho n}\rho)J_{2k}(k_0\rho\sin\theta)\rho d\rho\right]. \quad (14)$$

By means of the following Lommel integral formula:

$$\int_0^a xJ_p(k_m x)J_p(k_n x)dx = \frac{x}{k_m^2 - k_n^2}\left[J_p(k_m x)\frac{d}{dx}J_p(k_n x) - J_p(k_n x)\frac{d}{dx}J_p(k_m x)\right]\Big|_0^a, \quad (15)$$

the fact $J'_m(\chi_n) = J'_m(k_{\rho n}a) = 0$ implies that both integrations of (13) and (14) can be calculated as

$$\int_0^a J_{2(k-1)}(k_{\rho n}\rho)J_{2(k-1)}(k_0\rho\sin\theta)\rho d\rho = \frac{a}{k_{\rho n}^2 - k_0^2\sin^2\theta}\left[J_{2(k-1)}(k_{\rho n}a)J'_{2(k-1)}(k_0\rho\sin\theta)k_0\sin\theta - J'_{2(k-1)}(k_{\rho n}a)J_{2(k-1)}(k_0\rho\sin\theta)k_{\rho n}\right],$$

and

$$\int_0^a J_{2k}(k_{\rho n}\rho)J_{2k}(k_0\rho\sin\theta)\rho d\rho = \frac{a}{k_{\rho n}^2 - k_0^2\sin^2\theta}[J_{2k}(k_{\rho n}a)J'_{2k}(k_0\rho\sin\theta)k_0\sin\theta - J'_{2k}(k_{\rho n}a)J_{2k}(k_0\rho\sin\theta)k_{\rho n}].$$

Substituting them into (13) and (14), respectively, it is obvious to see that (16) and (17) hold. □

Similarly, for the even index $TE_{mn}$ mode, we have also the following result.

**Lemma 3.** *Under Cartesian coordinate system, if m is even, i.e., m = 2k, k = 1,2,3,..., then the plane-wave spectrum of* $TE_{mn}$ *mode is expressed as follows:*

$$\begin{aligned} f_x = & -\frac{jN_{mn}u^2 va\pi}{u^2 - v^2}\left\{(-1)^{k-1}\sin(2k-1)\phi'\left[J'_{(2k-1)}(v)\frac{J_{(2k-1)}(u)}{u} - J'_{(2k-1)}(u)\frac{J_{(2k-1)}(v)}{v}\right]\right. \\ & \left. -(-1)^k \sin(2k+1)\phi'\left[J'_{(2k+1)}(v)\frac{J_{(2k+1)}(u)}{u} - J'_{(2k+1)}(u)\frac{J_{(2k+1)}(v)}{v}\right]\right\}, \end{aligned} \quad (16)$$

$$\begin{aligned} f_y = & -\frac{jN_{mn}u^2 va\pi}{u^2 - v^2}\left\{(-1)^{k-1}\cos(2k-1)\phi'\left[J'_{2(k-1)}(v)\frac{J_{2(k-1)}(u)}{u} - J'_{2(k-1)}(u)\frac{J_{2(k-1)}(v)}{v}\right]\right. \\ & \left. +(-1)^k \cos(2k+1)\phi'\left[J'_{(2k+1)}(v)\frac{J_{(2k+1)}(u)}{u} - J'_{(2k+1)}(u)\frac{J_{(2k+1)}(v)}{v}\right]\right\}, \end{aligned} \quad (17)$$

*where* $u = k_{\rho n}a$, $v = k_0 a\sin\theta$.

In the sequel, according to (5), we will derive an orthogonal identity equation among plane-wave spectrum of different modes. For different mode index $m$, due to the orthogonal property of triangular function, the result, which is derived according to (5), of course, must be trivial. While for the same mode index $m$, $n$ is chosen $i$ and $j$, respectively, the fact $dk_x dk_y = \frac{1}{2}k_0^2 \sin 2\theta d\theta d\phi'$ implies that we can obtain the following result.

**Theorem 4.** *For two odd index modes $TE_{mi}$ and $TE_{mj}$, $m = 2k-1$, we have the following orthogonal integral identity equation:*

$$\int_{-\infty}^{\infty}\int_{-\infty}^{\infty}\vec{f}_{ti}(k_x,k_y)\cdot\vec{f}^{*}_{tj}(k_x,k_y)dk_xdk_y=\pi^3k_0^2a^2N_{mi}N_{mj}u_iu_j\int_0^{\frac{\pi}{2}}[B_{2(k-1)}(v,i)B_{2(k-1)}(v,j)+B_{2k}(v,i)B_{2k}(v,j)]\sin 2\theta d\theta=\begin{cases}1, & i=j\\ 0, & i\neq j\end{cases}, \tag{18}$$

*where*

$$B_{2(k-1)}(v,i)=\frac{1}{u_i^2-v^2}\left[vJ'_{2(k-1)}(v)J_{2(k-1)}(u_i)-u_iJ'_{2(k-1)}(u_i)J_{2(k-1)}(v)\right],$$

$$B_{2k}(v,i)=\frac{1}{u_i^2-v^2}\left[vJ'_{2k}(v)J_{2k}(u_i)-u_iJ'_{2k}(u_i)J_{2k}(v)\right].$$

Therefore, it is obvious to see, for two odd index modes $TE_{mi}$ and $TE_{mj}$, $m = 2k-1$, if $i \neq j$, that

$$\int_0^{\frac{\pi}{2}}[B_{2(k-1)}(v,i)B_{2(k-1)}(v,j)+B_{2k}(v,i)B_{2k}(v,j)]\sin 2\theta d\theta=0. \tag{19}$$

For example, especially, for $m = 1$, the electric field distribution $\vec{E}_a(x,y)$ of $TE_{1n}$ mode is expressed as follows:

$$\begin{aligned}E_x&=\frac{N_{1n}k_{\rho n}}{2}J_2(k_{\rho n}\rho)\sin 2\phi,\\ E_y&=\frac{N_{1n}k_{\rho n}}{2}[J_0(k_{\rho n}\rho)-J_2(k_{\rho n}\rho)\cos 2\phi],\end{aligned} \tag{20}$$

where $0 \leqslant \rho \leqslant a$, and $k_{\rho n}$ is the $n$th non-zero root of the equation $J'_1(k_{\rho n}a)=0$. So, according to above-mentioned analysis, we obtain that

$$\begin{aligned}f_{xn}&=-N_{1n}u_na\pi\sin 2\phi' B_2(v,n),\\ f_{yn}&=N_{1n}u_na\pi[B_0(v,n)+\cos 2\phi' B_2(v,n)].\end{aligned} \tag{21}$$

When $n = i, j$, and $i \neq j$, we obtain that

$$\int_0^{\frac{\pi}{2}}[B_0(v,i)B_0(v,j)+B_2(v,i)B_2(v,j)]\sin 2\theta d\theta=0. \tag{22}$$

## 4. The numerical method for determining components of different modes

From (5), it is obvious that far field plane-wave spectrums of open end circular waveguide are orthogonal with each other. By means of this orthogonal property, we can compute aperture components distribution of open end circular waveguide according to the testing value of plane-wave spectrums. However, it is necessary to use a lot of test data of plane-wave spectrums in the plane $R^2$. Later, [18] proposed an inner-product method. There, a radiation matrix was defined by using the inner-product, and modes components were determined by solving a system of linear equations. Since it was only necessary to compute the integral in two main axis, but not in the whole plane $R^2$, that method reduced the quantity of measurement data. Above-mentioned analysis was reasonable in theory. However, in real implementation, it would generate two problems:

(1) The scale and the framework of the system of linear equations were not known previously, since we did not know previously how many and which modes exist.
(2). Since the testing plane is bounded, the elevation angle $\theta$ in the linear integral is impossible to attain the upper boundary, and is truncated at $\theta = \theta_m$, there exists the truncation error.

Similar to the inner-product method in [18], we propose the following simple method to determine different modes components by solving a system of linear equations, under the same azimuthal angle index.

Suppose that there are $N$ character modes at the aperture of open-end circular wave-guide, then the far field radiation distribution can be expressed as follows:

$$\vec{E}(\theta,\phi')=\sum_{n=1}^{N}a_n\vec{f}_{tn}(\theta,\phi'), \tag{23}$$

where $a_n$ is the amplitude of the corresponding eigenmode.

For $\phi' = 0$ and $\phi' = \frac{\pi}{2}$, we multiply some existing plane-wave spectrum $\vec{f}_{tm}(\theta, \phi')$ at two sides of (23), and compute

$$\begin{aligned} F_{mn} &= \pi^3 k_0^2 \int_0^{\frac{\pi}{2}} \vec{f}_{tm}(\theta, \phi') \cdot \vec{f}_{tn}(\theta, \phi') \sin 2\theta d\theta, \\ E_m &= \pi^3 k_0^2 \int_0^{\frac{\pi}{2}} \vec{E}(\theta, \phi') \cdot \vec{f}_{tm}(\theta, \phi') \sin 2\theta d\theta, \end{aligned} \tag{24}$$

where $\vec{E}(\theta, \phi')$ in the second integral is replaced with the testing far field value. Therefore, similar to [18], we obtain the following system of linear equations about $a_n$:

$$[F_{mn}][a_n] = [E_m]. \tag{25}$$

Then, by solving (25), we can compute different modes components and their amplitudes at the aperture of open-end circular wave-guide.

Unlike [18], when we compute the inner-product, based on the integral identity equation (18) or (19), we use the weight function $\sin 2\theta$, and can overcome above-mentioned shortcomings.

For the sake of clarity, we introduce furthermore the proposed method, by considering the aperture field which consists of some $TE_{1n}$ modes.

Firstly, at the main axis $\phi' = 0$, from (21), we obtain that

$$\begin{aligned} F_{ij}^{y}\Big|_{\phi=0} &= \pi^3 k_0^2 \int_0^{\frac{\pi}{2}} f_{yi}(\theta) f_{yj}(\theta) \sin 2\theta d\theta \\ &= \pi^3 k_0^2 a^2 N_{1i} N_{1j} u_i u_j \left\{ \int_0^{\frac{\pi}{2}} [B_0(v,i)B_0(v,j) + B_2(v,i)B_2(v,j)] \sin 2\theta d\theta + \int_0^{\frac{\pi}{2}} [B_0(v,j)B_2(v,i) + B_0(v,i)B_2(v,j)] \sin 2\theta d\theta \right\}. \end{aligned} \tag{26}$$

According to the integral identity equation (22), we get that

$$F_{ij}^{y}\Big|_{\phi=0} = \pi^3 k_0^2 a^2 N_{1i} N_{1j} u_i u_j \int_0^{\frac{\pi}{2}} [B_0(v,j)B_2(v,i) + B_0(v,i)B_2(v,j)] \sin 2\theta d\theta. \tag{27}$$

Similarly, at the main axis $\phi' = \frac{\pi}{2}$, it holds that

$$F_{ij}^{y}\Big|_{\phi=\frac{\pi}{2}} = -\pi^3 k_0^2 a^2 N_{1i} N_{1j} u_i u_j \int_0^{\frac{\pi}{2}} [B_0(v,j)B_2(v,i) + B_0(v,i)B_2(v,j)] \sin 2\theta d\theta. \tag{28}$$

Obviously, we obtain that

$$F_{ij}^{y}\Big|_{\phi=0} + F_{ij}^{y}\Big|_{\phi=\frac{\pi}{2}} = 0. \tag{29}$$

(29) implies that it is possible to eliminate some intersectional integral items between two different modes. Thereby, it is simplified to solve (23) as follows:

$$a_n = \frac{\int_0^{\frac{\pi}{2}} \left[E_y(\theta, \phi' = 0) f_{yn}(v, \phi' = 0) + E_y\left(\theta, \phi' = \frac{\pi}{2}\right) f_{yn}\left(v, \phi' = \frac{\pi}{2}\right)\right] \sin 2\theta d\theta}{\int_0^{\frac{\pi}{2}} \left[f_{yn}^2(v, \phi' = 0) + f_{yn}^2\left(v, \phi' = \frac{\pi}{2}\right)\right] \sin 2\theta d\theta}. \tag{30}$$

Obviously, under the condition that we do not know previously how many and which modes exist, $a_n$ is also simple to compute according to (30), and it can reduce the truncation error, due to the using of $\sin 2\theta$.

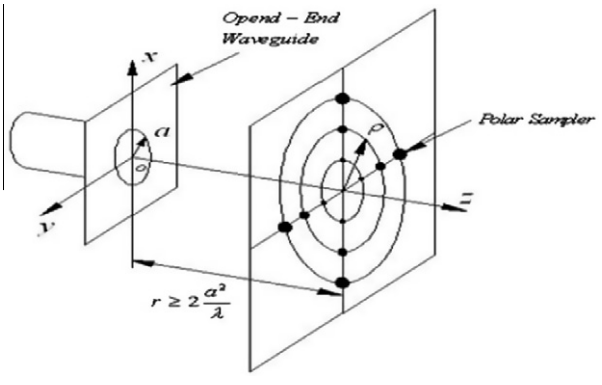


**Fig. 2.** The experimental set.

## 5. Numerical experiments

In this section, we carry out some numerical experiments to show that the method proposed in Sections 3 and 4 is efficient.

### 5.1. The experimental set

In order to show that the method is effective, we design the following testing device (see Fig. 2). The minimum distance from the sample place to the aperture of waveguide satisfies the FraunHoffr far field condition: $r \geqslant 2a^2\lambda$.

### 5.2. The experimental result

In the implementation, we choose the radius of open-end circular waveguide $a = 5\lambda$, where $\lambda$ is the wave length of the electromagnetic wave. Under the condition, we know that five modes $TE_{1i}$, $i = 1,\ldots,5$ can propagate through the waveguide. In addition, for the sake of normalization, we might as well assume $a_i = 1$, $i = 1,\ldots,5$.

Firstly, for five modes $TE_{1i}$, $i = 1,\ldots,5$, when $i = j$, and $i = 1,\ldots,5$, we point out the distribution of the radial angle for the integrand in (18) at Fig. 3.

According to Fig. 3, relatively, compared with the wave length, when the radius $a$ is larger, all of the majority amplitudes of plane-wave spectrums are distributed among some range with the elevation angle $\theta$. As the index of mode is increasing,

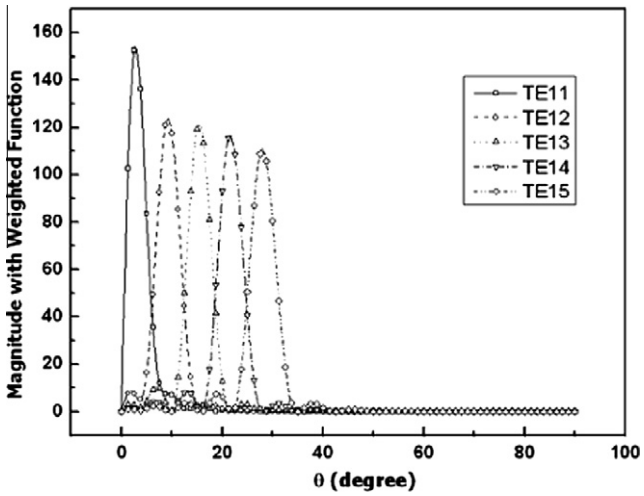


**Fig. 3.** The distribution of the radial angle for five modes $TE_{1i}$, $i = 1,\ldots,5$.

**Table 1**
The detail information for verifying the identity equation (18).

| Modes | $TE_{11}$ | $TE_{12}$ | $TE_{13}$ | $TE_{14}$ | $TE_{15}$ |
|---|---|---|---|---|---|
| $TE_{11}$ | 0.990964 | −0.002744 | −0.001783 | −0.001396 | −0.001212 |
| $TE_{12}$ | −0.002744 | 0.998997 | −8.41E-4 | −8.62E−4 | −9.66E−4 |
| $TE_{13}$ | −0.001783 | −8.41E−4 | 0.999118 | −0.001051 | −0.001295 |
| $TE_{14}$ | −0.001396 | −8.62E−4 | −0.001051 | 0.998652 | −0.001731 |
| $TE_{15}$ | −0.001212 | −9.66E−4 | −0.001295 | −0.001731 | 0.997728 |

**Table 2**
The detail information by computing the integral (27) with the traditional inner-product method.

| Modes | $TE_{11}$ | $TE_{12}$ | $TE_{13}$ | $TE_{14}$ | $TE_{15}$ |
|---|---|---|---|---|---|
| $TE_{11}$ | 0.171476 | −0.244664 | −0.151224 | −0.110018 | −0.08664 |
| $TE_{12}$ | −0.244664 | 0.92758 | −0.044957 | −0.032929 | −0.026184 |
| $TE_{13}$ | −0.151224 | −0.044957 | 0.971866 | −0.020859 | −0.016847 |
| $TE_{14}$ | −0.110018 | −0.032929 | −0.020859 | 0.984254 | −0.013055 |
| $TE_{15}$ | −0.08664 | −0.026184 | −0.016874 | −0.013055 | 0.988823 |

the elevation angle $\theta$ corresponding to the peak value of plane-wave spectrums is increasing, too. Moreover, there is some overlap for plane-wave spectrums between adjacent modes.

Secondly, we verify the identity equation (18) by using trapezoidal integration. The result is summarized in Table 1. As it is pointed out theoretically, when $i \neq j$, the numerical integral in (18) tends to zero, and the residual error is $10^{-3}$ approximately. So, according to the numerical result, the identity equation (18) is verified well.

Similarly, by using trapezoidal integration to compute the integral (27) with the traditional inner-product method, we obtain the corresponding result in Table 2.

According to the information in Tables 1 and 2, under the same condition, the residual error is fairly smaller for the effect on intersectional integral items among different modes of (18) than that of (27) with the traditional inner-product method.

Since intersectional integral items at two main axis $\phi' = 0$ and $\phi' = \frac{\pi}{2}$ may offset each other, it is verified that the method based on (30) is efficient to determine different $TE_{1n}$ modes components and their amplitudes at the aperture of open-end circular wave-guide.

## 6. Conclusion

It is the difficult work to discriminate the mode content at the plane of $z = 0$, by taking advantage of the plane-wave spectrum of the radiation of circular waveguide. Firstly, various methods for mode discrimination, analysis and their respective characteristics have been summarized in this paper. Then, by using the orthogonality of circular waveguide modes, an orthogonal integral identity equation is proposed among plane-wave spectrum of different modes, under the same azimuthal angle index. Moreover, based on this identity equation, a simple method is proposed to determine components of different modes. Finally, some numerical experiment results are also reported to verify that the method is efficient to determine different $TE_{1n}$ modes components and their amplitudes.

## Acknowledgement

The authors would like to thank two anonymous referees, whose constructive comments led to a considerable revision of the original paper. This work was supported in part by NNSF (Nos. 61071018 and 11061011) of China and Program for Excellent Talents in Guangxi Higher Education Institutions ([2009]156).

## References

[1] M.P. Forrer, K. Tomiyasu, Determination of higher order propagating modes in waveguide systems, J. Appl. Phys. 29 (1958) 1040–1045.
[2] H.W. Glock, U.V. Rienen, An iterative algorithm to evaluate multimodal S-parameter measurements, IEEE Trans. Magnet. 36 (2000) 1841–1845.
[3] D.J. Lewis, Mode couplers and multimode measurement techniques, IEEE Trans. Microw. Theor. Tech. 7 (1959) 110–116.
[4] C. Seguinot, P. Kennis, J.F. Legier, F. Huret, E. Paleczny, L. Hayden, Multimode TRL-A new concept in microwave measurements: theory and experimental verification, IEEE Trans. Microw. Theor. Tech. 46 (1998) 536–542.
[5] W.X. Wang, Y.B. Gong, G.F. Yu, L.N. Yue, J.H. Sun, Mode discriminator based on mode-selective coupling, IEEE Trans. Microw. Theor. Tech. 51 (2003) 55–63.
[6] J.M. Baird, D.H. Roper, R.W. Grow, Surface array waveguide mode analyzer, IEEE MTT-S Int. Microw. Symp. Dig. 1 (1992) 137–140.
[7] R.H. Johnston, Measurement of modes in an overmoded circular waveguide, in: Proceedings of the 40th Midwest Circuits and Systems Symposium, vol. 1, 1998, pp. 599–602.
[8] P.V. Nikitin, D.D. Stancil, A.G. Cepni, A.E. Xhafa, O.K. Tonguz, D. Brodtkorb, A novel mode content analysis technique for antennas in multimode waveguides, IEEE Trans. Microw. Theor. Tech. 51 (12) (2003) 2402–2408.
[9] Z.X. Zhang, A method lor identifying gyrotron output mode compositions, Acta Electronica Sinica (1985) 45–50.
[10] Z.X. Zhang, G. Janzen, G. Muller, P.G. Schuller, M. Thumm, R. Wilhelm, V. Erckmann, Mode analysis of gyrotron radiation by far field measurements, in: Conference Digest 8th International Conference on Infrared and Millimeter Waves, Miami Beach, FL, USA, paper T43, 1983.
[11] R.J. Vernon, W.R. Pickles, M.J. Buckley, F. Firouzbakht, J.A. Lorbeck, Mode content determination i n over-moded circular waveguides by open-end radiation pattern measurement, IEEE AP-S Int. Symp., Blacksburg, Virginia (1987) 222–225.
[12] D.S. Stone, Mode analysis in multimode waveguides using voltage traveling wave ratios, IEEE Trans. Microw. Theor. Tech. 29 (2) (1981) 91–95.
[13] N.L. Aleksandrov, A.V. Chirkov, G.G. Denisov, S.V. Kuzikov, Mode content analysis from intensity measurements in a few cross sections of oversized waveguides, Int. J. Infrared Millimeter Waves 18 (8) (1997) 1505–1516.
[14] W. Kasparek, G.A. Muller, The wavenumber spectrometer – an alternative to the directional coupler for multimode analysis in oversized waveguides, Int. J. Electron. 64 (1) (1988) 5–20.
[15] M.K. Thumn, W. Kasparek, Passive high-power microwave components, IEEE Trans. Plasma Sci. 30 (3) (2002) 755–786.
[16] W.X. Wang, L.N. Yue, G.Q. Zhao, Y.B. Gong, Discrimination and analysis of microwave modes in high power systems, Int. J. Infrared Millimeter Waves 26 (2) (2005) 147–161.
[17] V.I. Malygin, A.B. Paveljev, Determination of the mode content in spurious microwave radiation of the gyrotron with a straight axisymmetric output, Int. J. Infrared Millimeter Waves 20 (1) (1999) 33–56.
[18] J.A. Lorbeck, R.J. Vernon, Determination of mode content and relative phase in highly overmoded circular waveguides by open-ended radiation pattern measurement, IEEE AP-S Int. Symp. 3 (1989) 1251–1254.
[19] R.E. Collin, Antennas and Radio Wave Propagation, McGraw-Hill, NY, 1985.
[20] R.C. Rudduck, D.F. Wu, M.R. Intihar, Near-field analysis by the plane-wave spectrum approach, IEEE Trans. Antenn. propagat. 21 (5) (1973) 231–234.
[21] N. Marcuvitz, Waveguide Handbook, McGraw-Hill, NY, 1951.